Novel technologies for greenfield exploration
Edited by Pertti Sarala
Geological Survey of Finland, Special Paper 57, 155–172, 2015

AUDIOMAGNETOTELLURIC (AMT) MEASUREMENTS: A NEW TOOL FOR MINERAL EXPLORATION AND UPPER CRUSTAL RESEARCH AT THE GEOLOGICAL SURVEY OF FINLAND

by
Ilkka Lahti

Lahti, I. 2015. Audiomagnetotelluric (AMT) measurements: A new tool for mineral exploration and upper crustal research at the Geological Survey of Finland. *Geological Survey of Finland, Special Paper 57*, 155–172, 17 figures.

The audiomagnetotelluric (AMT) sounding technique is used to obtain information on the electrical conductivity of the bedrock and it can be used therefore in the search for conducting mineral deposits such as massive sulphides. In 2011, new tensor instruments with two broadband electromagnetic (EM) receivers and necessary sensors for both high-frequency AMT and low-frequency magnetotelluric (MT) surveys were acquired by the Geological Survey of Finland (GTK). The instruments have been used in several target-scale AMT surveys where the depth of interest is from about 300 m to 2 km and the site spacing from 150 m to 1 km.

This paper presents practical aspects of AMT surveys such as investigating the effects of diurnal variations in AMT source field intensity, the removal of man-made electromagnetic disturbances, the required duration of measurement, and generally performing surveys effectively. Another challenge that particularly relates to the frequencies utilized in AMT is the low signal strength at 1000–5000 Hz, which was also examined in the subtask. 3D forward modelling of AMT array data was also carried out.

Field tests revealed that 15 min is an adequate duration for time series recording for good AMT data in the frequency range of 1–10 000 Hz. The use of a remote reference proved essential in the entire AMT frequency range. AMT instruments should record during the night in order to achieve good quality data in the frequency band of 1000–5000 Hz. To enable effective surveying, two field crews were trained, several practical field protocols were justified, and equipment was tailored in the project. To speed up measurements, metal sticks were tested as electrodes.

A field example is presented that illustrates AMT array data from the Rovaniemi area, northern Finland. The data are visualized as sounding curves and maps. A 3D forward modelling study was carried out to model Tipper responses and off-diagonal elements of the impedance tensor.

Keywords (GeoRef Thesaurus, AGI): geophysical methods, magnetotelluric methods, audiomagnetotelluric methods, electrical conductivity, mineral exploration, Rovaniemi, Finland

Geological Survey of Finland, P.O. Box 77, FI-96101 Rovaniemi, Finland

E-mail: ilkka.lahti@gtk.fi

BACKGROUND

In the audiomagnetotelluric (AMT) method, the electrical conductivity structure of the subsurface is imaged by using Earth's natural electromagnetic (EM) fields as a source (e.g. Berdichevsky & Dmitriev 2008). The principles of the technique were first introduced by Tikhonov (1950) and Cagniard (1953). In AMT, the primary incident EM fields are considered as planar in geometry and propagating vertically downward. In the earth, EM waves travel diffusively so that high-frequency (short wavelength) waves penetrate a relatively short distance, while low-frequency (long wavelength) waves reach greater depths. The main advantage of AMT is the wide survey depth range from hundreds of metres down to several kilometres. The magnetotelluric method (MT) uses even lower frequencies and the survey depth can therefore even be hundreds of kilometres.

AMT-MT measurement requires a simultaneous time series of orthogonal components of magnetic (B_x, B_y and B_z) and electric (E_x and E_y) fields resulting from large-scale solar-driven ionospheric and magnetospheric electric currents. The energy sources for frequencies above 1 Hz are EM waves caused by distant lightning storms and they propagate within the Earth–ionosphere waveguide (Garcia & Jones 2002). A schematic diagram of the audio-magnetotelluric site is presented in Figure 1. Magnetic field time series are recorded using induction coil magnetometers placed perpendicularly on the ground. Electric field time series are recorded in two orthogonal directions using electrodes. A GPS receiver is a standard part of the modern geophysical system. It provides accurate timing and is needed for synchronization between simultaneous remote referenced sites, as well as for the determination of the exact site location. Data are usually collected on high precision, high dynamic range data loggers having a 24-bit ADC (Smirnov et al. 2008).

In the frequency domain, a linear relationship exists between the measured horizontal components of the EM field, i.e. the measured magnetic and electric field components. This relationship can be mathematically represented by two linear equations. By assuming plane wave excitation, orthogonal components of B and E are linearly related through the complex impedance tensor **Z** (Berdichevsky & Dmitriev 2008)

$$\begin{bmatrix} E_x \\ E_y \end{bmatrix} = \begin{bmatrix} Z_{xx} & Z_{xy} \\ Z_{yx} & Z_{yy} \end{bmatrix} \begin{bmatrix} B_x \\ B_y \end{bmatrix} \quad (1)$$

Complex off-diagonal impedances Z_{xy} and Z_{yx} at a varying frequency are usually graphically shown as apparent resistivity and phase curves. Geomag-

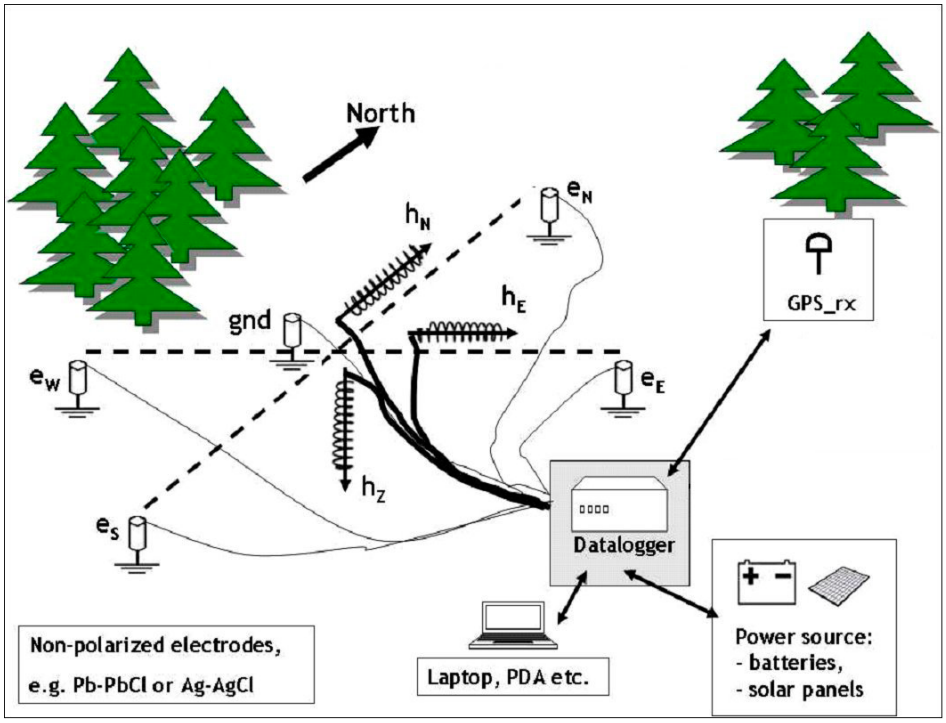

Fig. 1. Schematic diagram of an AMT-MT measurement site (modified from Smirnov et al. 2008).

netic depth sounding also requires the measurement of the vertical magnetic field B_Z, which is related to the horizontal magnetic fields B_x and B_y through the vector

$$[B_z] = \begin{bmatrix} T_{zx} & T_{zy} \end{bmatrix} \begin{bmatrix} B_x \\ B_y \end{bmatrix} \quad (2)$$

For an isotropic layered (1D) Earth, the diagonal elements Z_{xx} and Z_{yy} are zero in equation (1) and $Z_{xy} = - Z_{yx}$. In the case of an isotropic two-dimensional (2D) Earth, conductivity changes with depth and one horizontal dimension. In this case, the tensor can be rotated to the coordinate system where observed electric and magnetic fields are parallel and orthogonal to the structure. In this rotated coordinate system, Z_{xx} and Z_{yy} are again zero, but the magnitude of Z_{xy} is generally not the same as Z_{yx}. Z_{xy} and Z_{yx} define transverse electric (TE) and transverse magnetic (TM) modes. For 3D structures, generally none of the tensor components are zero (Heinson & White 2005). The theoretical framework of the method is extensively presented in Berdichevsky & Dmitriev (2008).

In addition to numerous conference abstracts, the use of AMT in mineral exploration has been reported by Strangway et al. (1973), Lakanen (1986), Farquharson & Craven (2008), Tuncer et al. (2006) and Türkoglu et al. (2009). Wannamaker & Doerner (2002) used MT soundings in north-eastern Nevada to study the crustal structure of the Ruby Mountains and the southern Carlin mineral trend, which holds world-class gold deposits. The challenges related to the natural source field at AMT frequencies have been discussed by Garcia & Jones (2002).

AMT MEASUREMENTS AT THE GEOLOGICAL SURVEY OF FINLAND

AMT surveys have previously been carried out by GTK using scalar equipment (e.g. Lanne 2000), but the acquisition of tensor data started in 2009 (Fig. 2). The first such survey was arranged in the Kittilä Greenstone Belt area in co-operation with the University of Oulu (Lahti et al. 2012a, Lahti et al. 2012b). The measurements (Fig. 3a) were mainly conducted along the reflection seismic profiles FIRE4A and 4B using instruments manufactured at Uppsala University. The data frequency range of the Uppsala instruments is from about 500 Hz to 0.001 Hz. Due to the wide measured frequency band, the survey could be considered as a broadband MT (BMT) survey, as it covered both MT and AMT frequencies. A detailed description of the used instruments has been provided by Smirnov et al. (2008). Figure 3(a) shows the location of the Kittilä MT sites on the geological map of the study area. The acquired dataset consists of data from 80 sites with a spacing of 500 m to 4 km. Prior to inversions, the data were analysed for regional strike and dimensionality. 2D conductivity models were obtained by inverting the determinant of the impedance tensor (Siripunvaraporn & Egbert 2000, Pedersen & Engels 2005) and TE and TM data jointly using the nonlinear conjugate gradient algorithm of Rodi & Mackie (2001). Figure 3(b) presents determinant 2D models in a 3D perspective view together with FIRE reflection seismic results.

As the experiences of the Kittilä survey were promising, new AMT instruments with sensors adequate for mineral exploration were purchased in 2011. These include two broadband Metronix EM receivers and corresponding sensors to per-

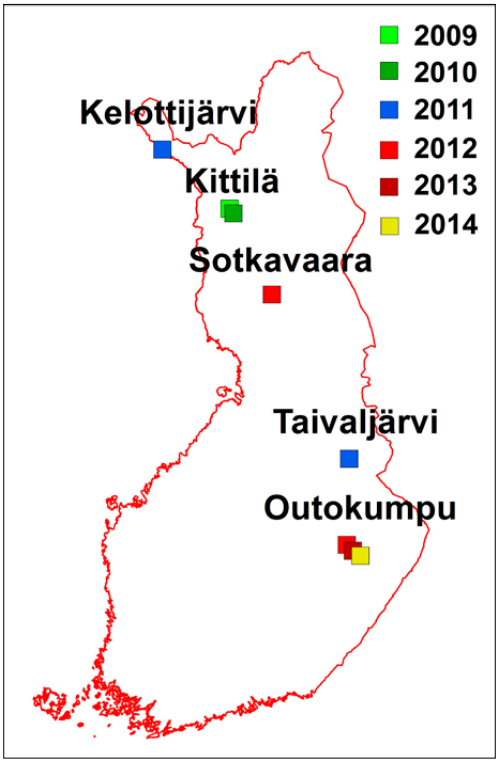

Fig. 2. Tensor AMT measurements by GTK since 2009.

form AMT surveys. Two receivers are necessary in order to have a simultaneous reference signal from a site established far from the survey area. The purchased high-frequency induction coil magnetometers (MFS-07) cover a wide frequency range from 0.001 Hz up to 50 kHz and can also be used for standard MT applications. Figure 4 displays one of the devices. In 2011, new instruments were implemented in the Kelottijärvi area, northern Finland. Since the first experiment in Kelottijärvi, AMT

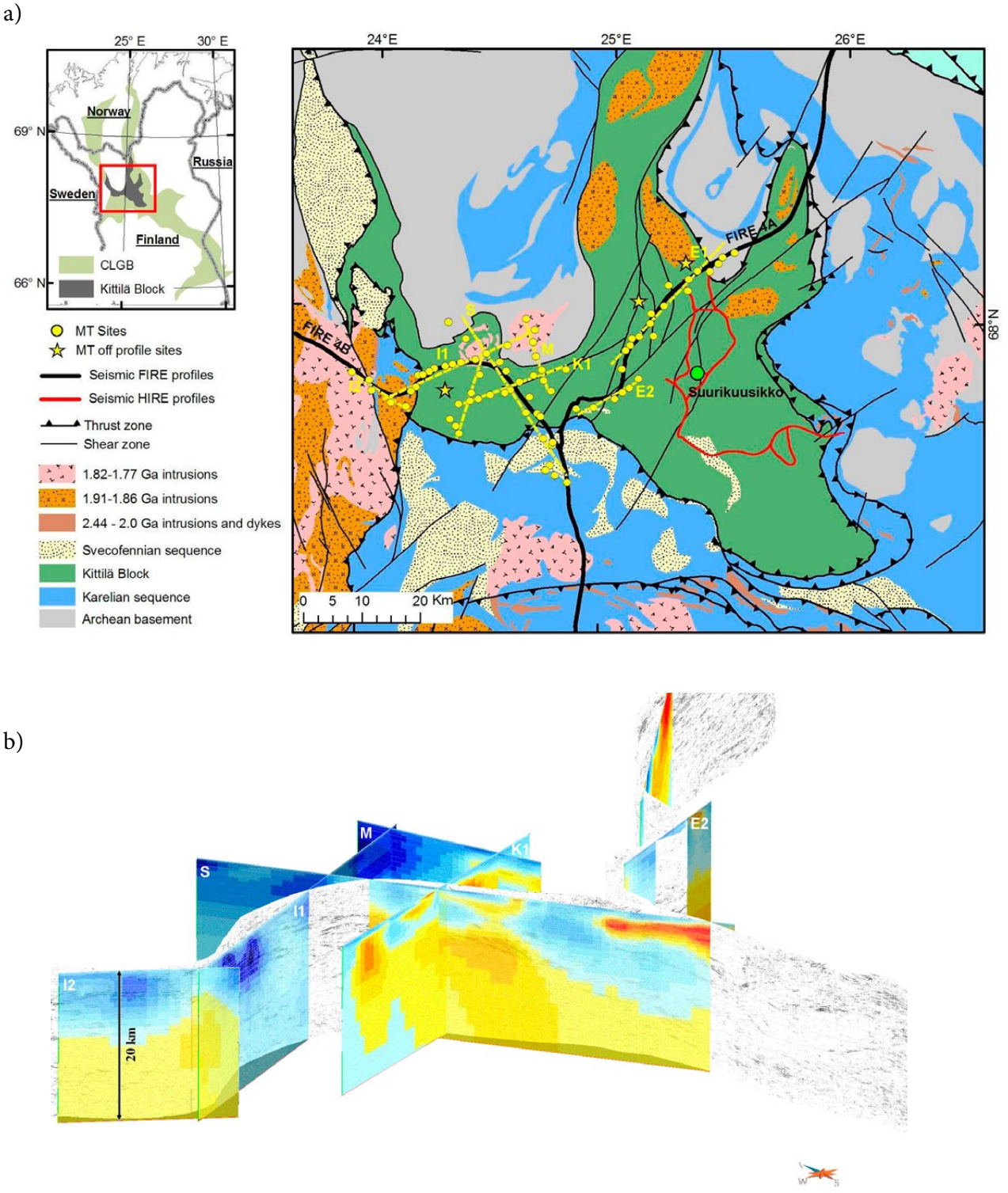

Fig. 3. MT survey in the Kittilä Greenstone Belt, northern Finland (2009–2010). a) Location of MT sites on the geological map of the study area. b) 2D smooth inversion models in 3D perspective view together with FIRE reflection results. Red colours show good conductors in the area. Bedrock map (Bedrock of Finland – DigiKP).

measurements have been performed in Taivaljärvi (2011), Sotkavaara (2012) and in the Outokumpu area (2012–2014). A prerequisite for quality measurements is skilled field personnel. Two field crews were trained during the surveys. The results of the Sotkavaara survey are discussed later in this paper.

Fig. 4. New AMT-MT equipment used at GTK.

PRACTICAL ASPECTS OF MEASUREMENTS

The main focus of this paper is on the practical measurement, processing and modelling routines of target-scale surveys. Effective surveying is essential, as measurements are time consuming in comparison to other electromagnetic sounding techniques. Therefore, the optimal duration of a measurement was investigated to obtain data in the frequency range of 1–10 000 Hz. The low intensity of the natural source electromagnetic field at 1000–5000 Hz is a challenge, particularly for AMT measurements. The signal strength is dependent on the time of day, and better results are usually obtained during night time and early morning hours. Man-made electromagnetic disturbances may cause errors in the processed sounding curves. A remote reference technique was applied to remove man-made distortions in AMT frequencies. A comparison of results using steel and non-polarizing electrodes was also carried out.

Remote reference (RR) technique in high-frequency AMT recordings

To improve data quality in areas of man-made EM noise, the use of the remote reference (RR) technique in time series recording is recommended (Gamble et al. 1979). Although RR is a standard tool in MT, its use in high-frequency AMT has not been widely reported. The principle of the RR technique is to record magnetic time series at some distant site simultaneously with the actual survey. The remote reference site needs to be located in an area with no man-made EM noise. During data processing, time series are correlated with the remote reference site, which helps to reduce uncorrelated noise. Therefore, it is important to obtain accurate timing for both sites, which is accomplished by GPS signal timing. We tested remote reference processing for AMT data and it proved to be generally essential in all surveys. Figure 4 presents single site and remote reference processed results for a site distorted by artificial EM noise. Although data estimates close to 50 Hz are still relatively poor, RR processed curves are generally better.

Optimizing the duration of a measurement

The main factor affecting the duration of AMT measurement is the recording time. When measurements started in 2011, 60-min recordings were performed. It soon became obvious that the recording length could be drastically shortened, especially as the frequency range of interest is 1–10 000 Hz. The recording time was first reduced to 40 min and then further to 30 min in 2012. In 2013, even shorter time series of recording times were assessed. Figure 6 shows the effect of recording time on the processed apparent resistivity and phase curves. The displayed recording times are 15 min, 5 min, 2 min and 1 min. At the frequencies shown in these images, it is clear that the recording time could be quite safely reduced from 30 min to 15 min, as the difference between 15 min and 5 min is still negligible. The lack of data becomes obvious in 2-min and 1-min recordings if frequencies less than 100 Hz are acquired. However, data estimates for more than 100 Hz are reasonable, even for a 1-min recording time.

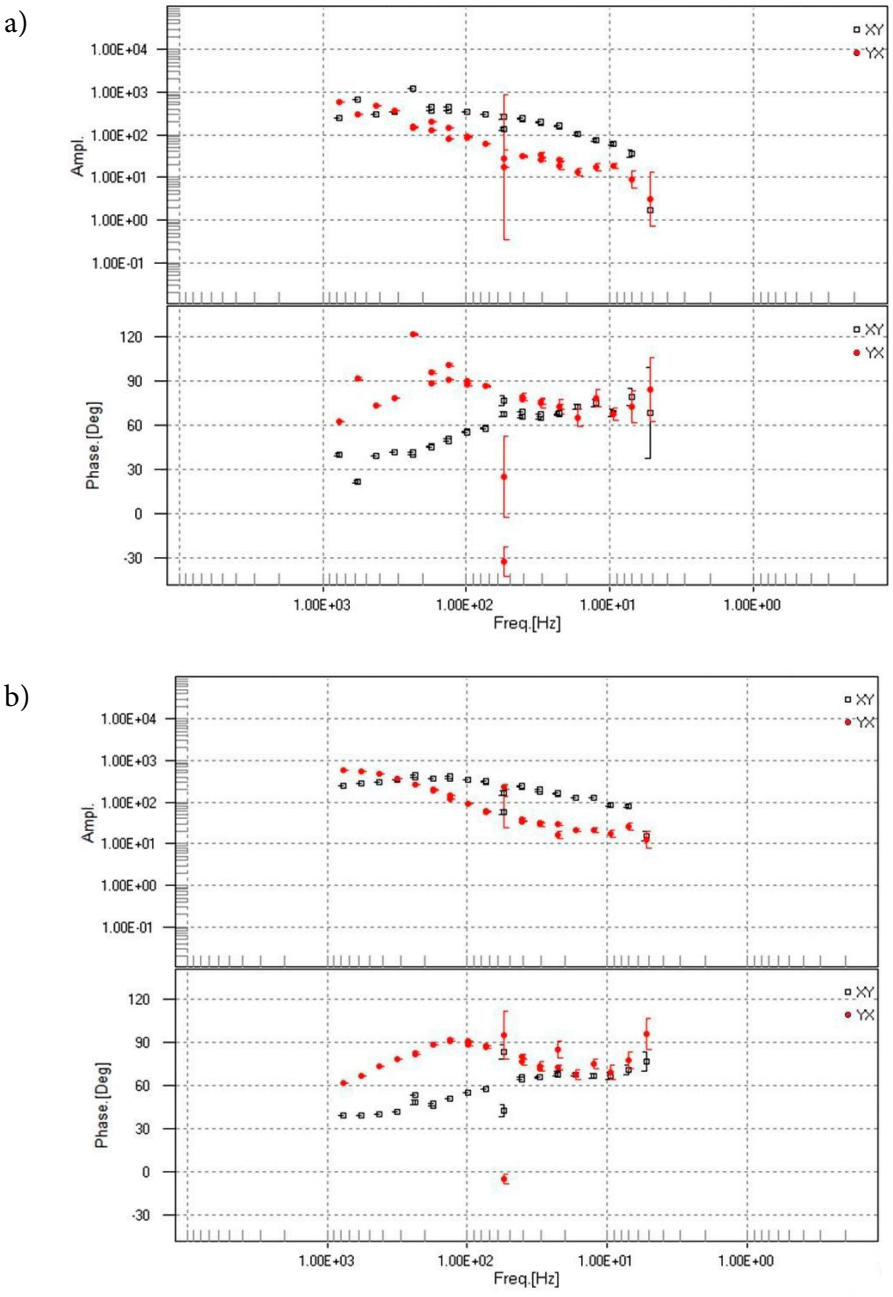

Fig. 5. AMT sounding curves using a) single site and b) remote reference processed time series data. Data quality is significantly improved using the remote reference processing technique. The data were recorded in the Outokumpu area in 2012.

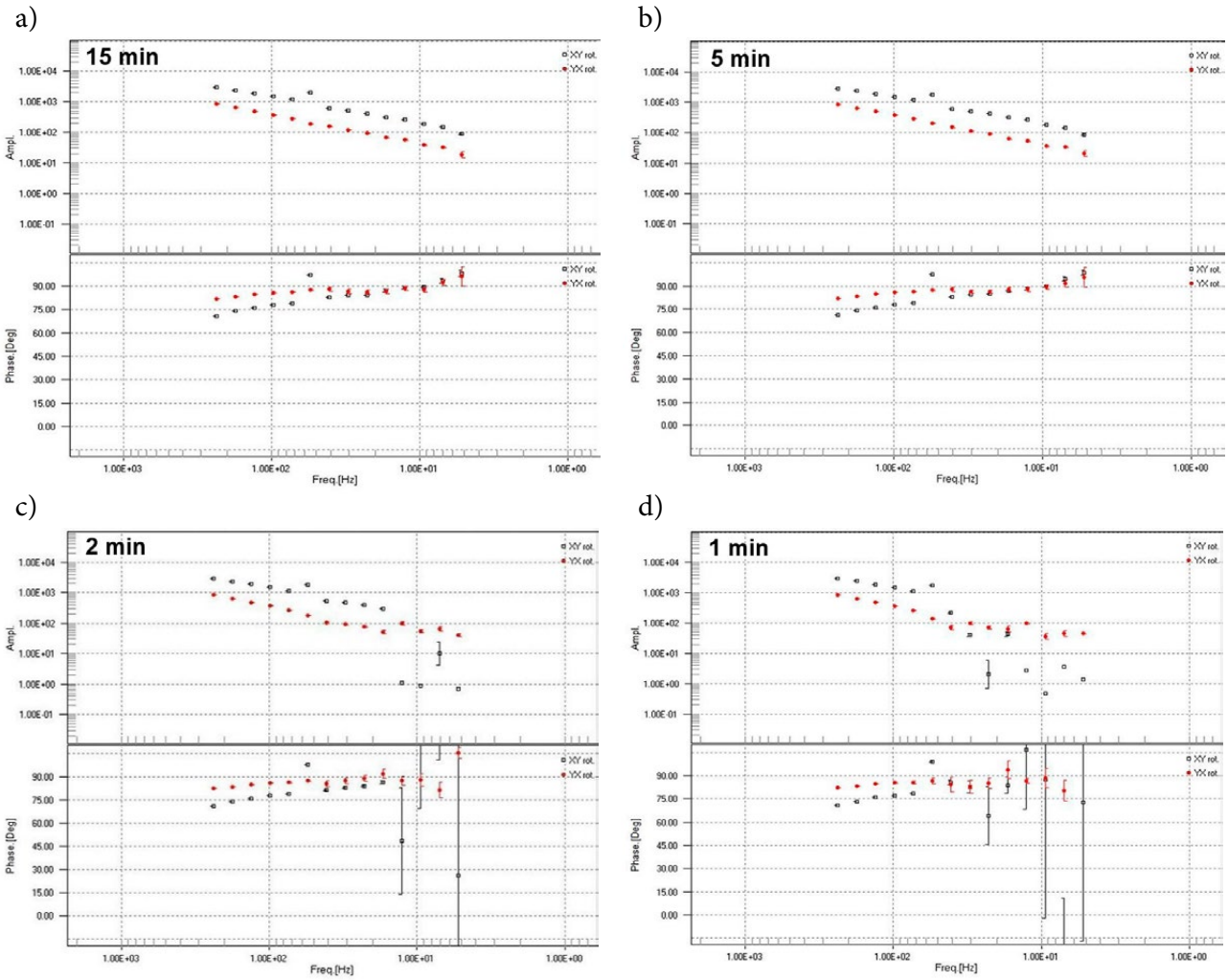

Fig. 6. Influence of recording time on AMT sounding curves: a) 15 min, b) 5 min, c) 2 min, d) 1 min.

Comparison of daytime and night-time measurements

The primary EM fields for frequencies (>1 Hz) are EM waves caused by distant thunderstorms (lightning). These waves propagate within the Earth–ionosphere waveguide. According to Garcia & Jones (2002), this waveguide has diurnal, seasonal and 11-year solar-cycle fluctuations, and these temporal fluctuations cause significant signal amplitude attenuation variations, especially at frequencies from 1000–5000 Hz that form the so-called AMT dead band. Thus, one problem associated with applying the AMT method to depths of less than 3 km can be the lack of signal in certain frequency bands during the desired acquisition interval. Analyses carried out by Garcia & Jones (2002) have demonstrated that the magnetic field signal levels are often below the coil noise threshold in the AMT dead band. In contrast, night-time signal levels are usually strong enough to also provide good estimates of the data at AMT dead-band frequencies.

Observations on diurnal variations in AMT source field signal levels were made in the project. The night is usually a good period to take measurements, because the EM field is less attenuated on the night side of the Earth–ionosphere waveguide. Modern AMT instruments are easily programmable to measure at selected time intervals. Figure 7 presents day and night data from the same site. The difference in quality is particularly seen in the AMT dead band (~1000–5000 Hz), and during the night the quality is clearly better. These data clearly show the importance of organizing AMT surveys so that recording during the night is possible. Another benefit is that longer acquisition enables low frequency MT data to be obtained, which allows deeper structures to be studied. Good daytime AMT data were mainly acquired in the frequency range of 1–1000 Hz and 5000–10000 Hz.

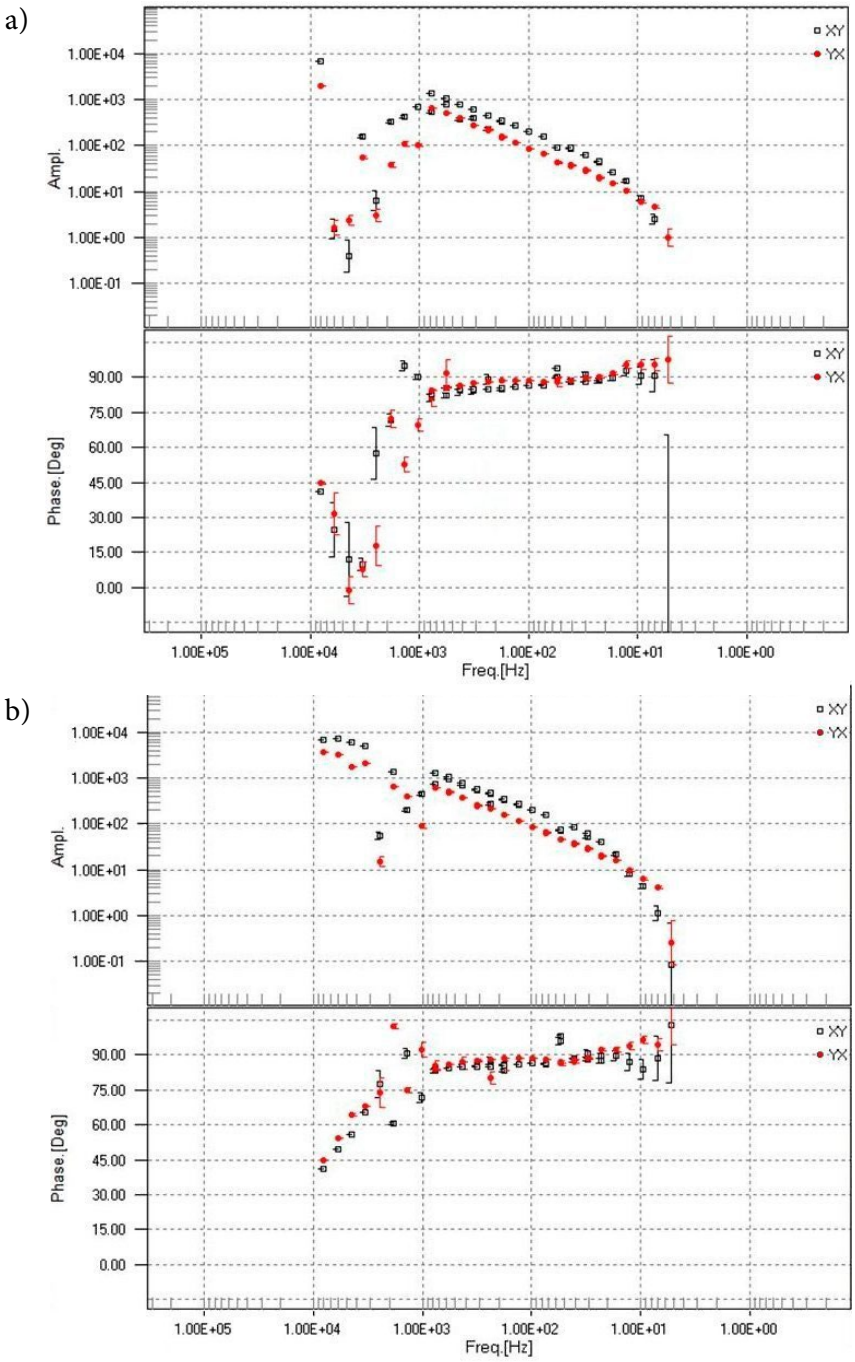

Fig. 7. Diurnal variation in AMT sounding curves from the same site: a) daytime and b) night-time measurement. The data were obtained in the Rovaniemi area in 2012.

Electrodes

The setting up of an AMT-MT site includes, among other procedures, installation of the induction coil magnetometers in three perpendicular orientations. As the coils should be placed on stable ground, they are usually dug in the ground. Measuring the vertical component of the magnetic field requires an even deeper pit. The placement of electrodes takes some time, as they have to be oriented according to magnetometers usually in a geomagnetic N–S, E–W direction. Non-polarizing electrodes are installed in the ground and saline fluid is usually added to reduce the contact resistance below 20 kΩ, as higher contact resistances result in a loss of signal in electric channels. The contact resistances are measured using a simple multimeter. To avoid digging pits and thereby speed up preparation of the site, we tested metal sticks. Figure 8 shows the non-polarizing electrode type (Pb-$PbCl_2$) and the metal stick used in the measurements. In very low frequency measurements, the polarization effects are assumed to cause noise in electric field signals, but at higher frequencies they are generally assumed to be negligible.

Both electrode types were used in the project. Time series recordings during the daytime were performed in the same place. First, metal spikes were tested by recording for 30 min. After that, non-polarizing electrodes were used in the same place. Time series were processed and the sounding curves are presented in Figure 9. The results show no significant differences in processed sounding curves at these frequencies, suggesting that metal sticks could be used in AMT measurements. However, this result needs to be confirmed by more extensive testing, because polarization effects can be difficult to recognize.

Fig. 8. Electrode types used in the measurements. a) A non-polarizing Pb-$PbCl_2$ electrode and b) a metal stick.

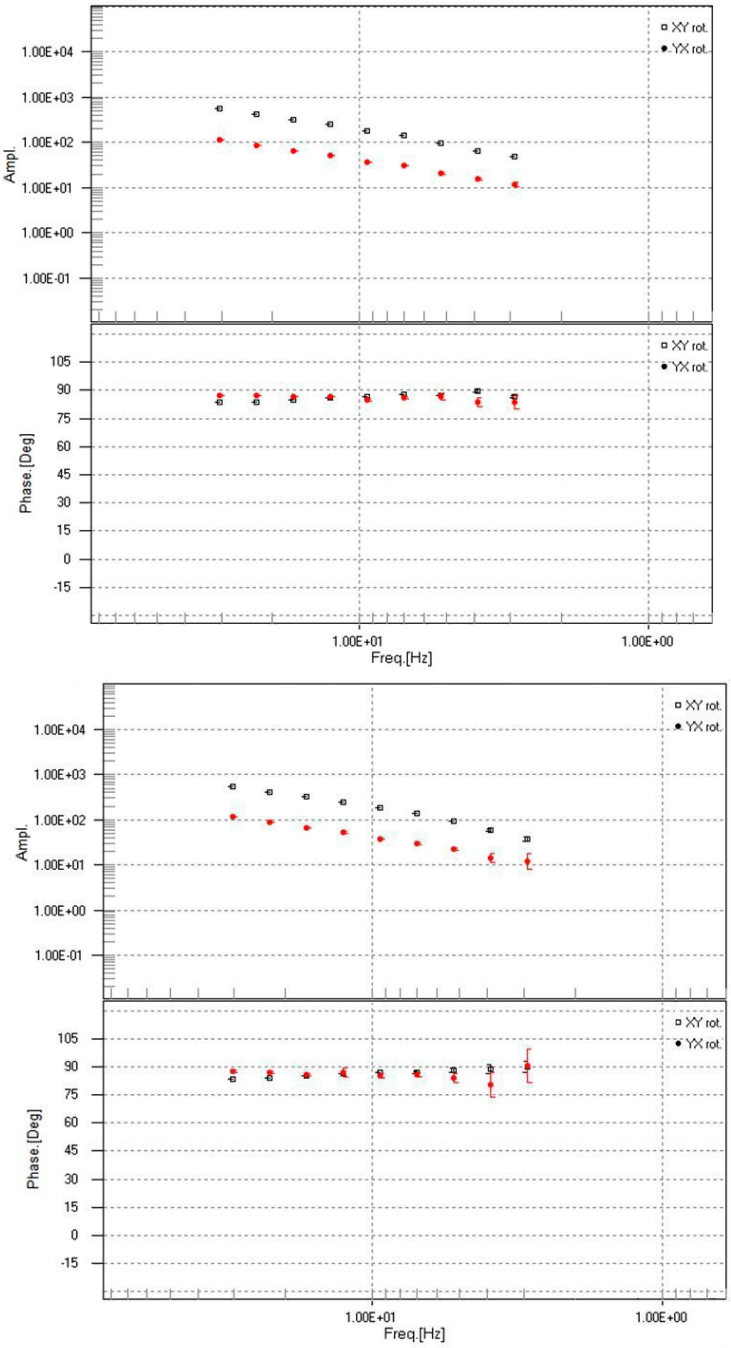

Fig. 9. Influence of electrode types on AMT data: a) apparent resistivity and phase using non-polarizing Pb-$PbCl_2$ electrodes and b) metal spikes.

TARGET-SCALE AMT MEASUREMENTS

In the following, a field example using GTK's new AMT instruments is presented. Measurements were carried out in the Sotkavaara intrusion area, which is located close to Rovaniemi. The survey aimed to image shallow subsurface conductivity structures at the depth of 100–700 m. Thus, the frequency range of 1–10 000 Hz and site spacing of 150–300 m were used.

Sotkavaara intrusion

The pyroxenitic Sotkavaara intrusion is located 25 km E-SE from Rovaniemi, Northern Finland, at 66.458°, 26.267° (Fig. 10). The intrusion belongs to the so-called Kuluskaira area of the Peräpohja schist belt. The 1.5 x 2.5 km pyroxenite body was intruded into the sulphide-bearing metasedimentary and volcanic rocks, thus being a favourable S source for mineralization in mafic-ultramafic magma. The host rocks of the intrusion contain some black schists, which are visible as conductors on aerogeophysical maps (Törmänen et al. 2014).

The presence of a mafic-ultramafic body intruding black schist-bearing rocks prompted investigations, which began in 2007 with outcrop sampling followed by ground geophysical surveys in 2008. As the intrusion was considered to be potential for Cu-Ni-PGE mineralizations, two holes (R398-R399) were drilled through the intrusion in 2009. These drillings revealed that the pyroxentic part of the intrusion is only ca. 300 m thick, followed by an up to 100-m-thick gabbro-amphibolite zone, and finally quartz-feldspar and mica schist of the Peräpohja schist belt. The second hole (R399) intersected a ca. 25-cm-thick massive sulphide vein containing 2.1% Ni, 0.47% Cu, 0.26% Co and trace amounts of PGEs (79 ppb Pd). To investigate the presence of additional massive sulphides, 7 holes (1272 m) were drilled in the central and marginal parts of the intrusion in 2012. These did not intersect any additional massive or disseminated sulphides. (Törmänen et al. 2014).

In addition to GTK's standard airborne geophysical measurements, ground magnetic, gravity, very low frequency resistivity (VLF-R), induced polarization (IP), Gefinex 400S (Sampo) and AMT measurements have been conducted in the Sotkavaara intrusion area. Borehole DC resistivity (mise-a-la-masse) measurements were also conducted in two drillholes in 2013. The intrusion is clearly detected in the airborne magnetic map as anomaly maximum (Fig. 10a). The airborne electromagnetic map suggests conductors close to and around the intrusion (Fig. 10b).

In 2011, an AMT array was measured in the area. The site spacing of the survey was 150–300 m, and altogether 37 sites were measured. The quality of the data was very good, as the study area is located in a distant area far from cultural electromagnetic disturbances. Figure 11 shows the array on the ground VLF-R apparent resistivity and phase maps. The VLF-R data were acquired with a Geonics EM16R receiver. In practice, the VLF-R response is same as the AMT response, but only with single polarization and at a very high frequency (23 kHz). Because of the high frequency, the VLF-R method maps the surface conductivity structure and, consequently, overburden usually influences the results.

Drillhole R399 in the central part of the intrusion intersected a 25-cm-thick massive sulphide vein at the depth of 252 m. However, it is still unclear whether the VLF-R impedance phase anomaly in the central part of the array (Fig. 11b) is related to the mineralization. Although drillholes R5 and R6 are located on the VLF-R phase anomaly, they do not intersect massive sulphides or other conductors. In turn, drillings have shown that conductivity anomalies surrounding the intrusion are due to graphitic schists.

Typical AMT sounding curves from the survey are presented in Figure 12. As seen in the figure, the data quality is generally very good, except in the frequency range of 1000–5000 Hz (AMT dead band). For this frequency range, data interpolation has been used. Measured phases are lower, typically 30–60°, at high frequencies, but increase with decreasing frequency and reach high values of about 80–90° at frequencies of less than 1000 Hz. Meanwhile, apparent resistivity values decrease with decreasing frequency. In general, qualitative (1D) interpretation of these curve types shows a highly resistive uppermost intrusion and enhanced conductivity at greater depths.

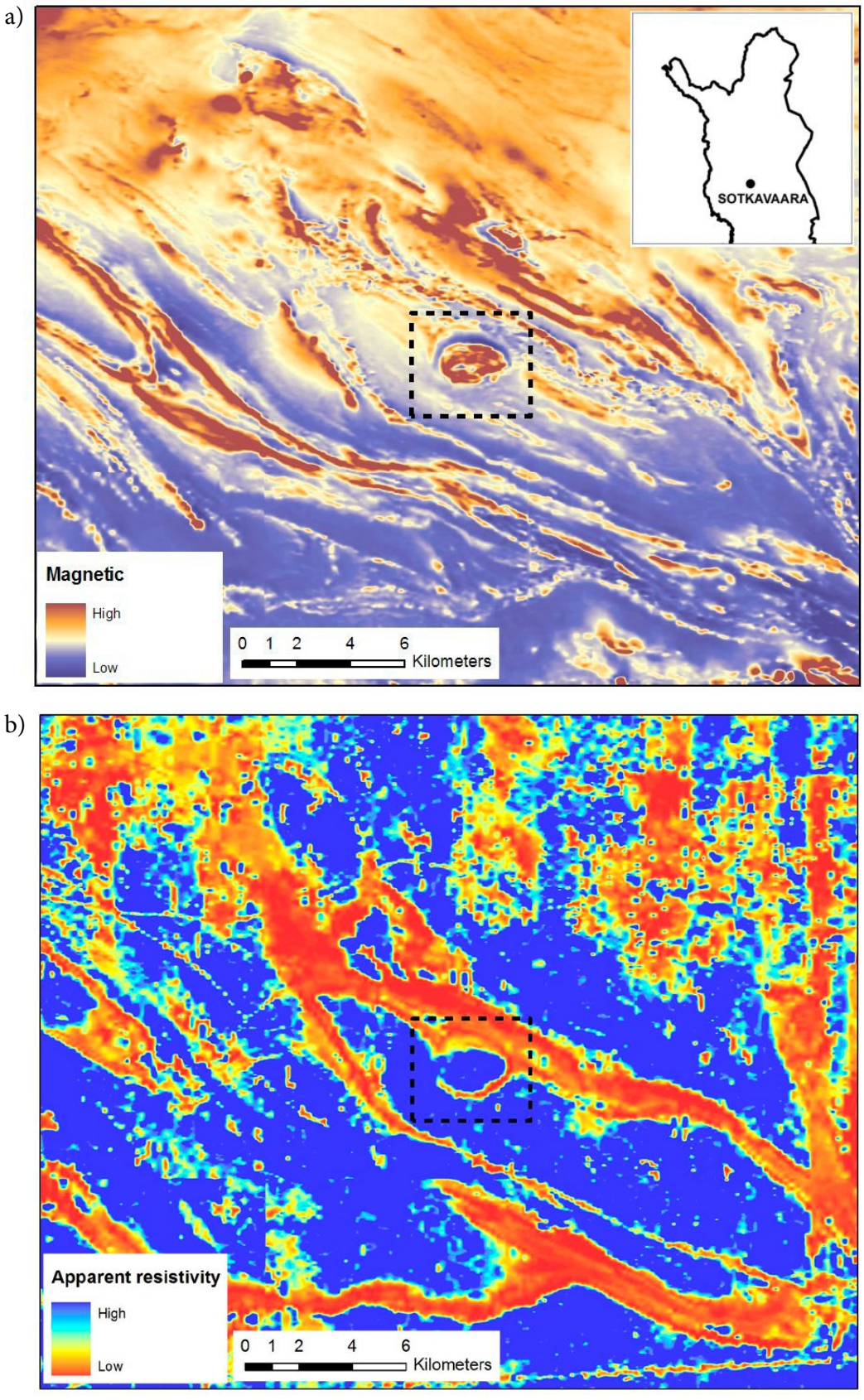

Fig. 10. Airborne (a) magnetic and (b) electromagnetic maps of the Sotkavaara intrusion area. The dashed line shows the location of the oval-shaped intrusion.

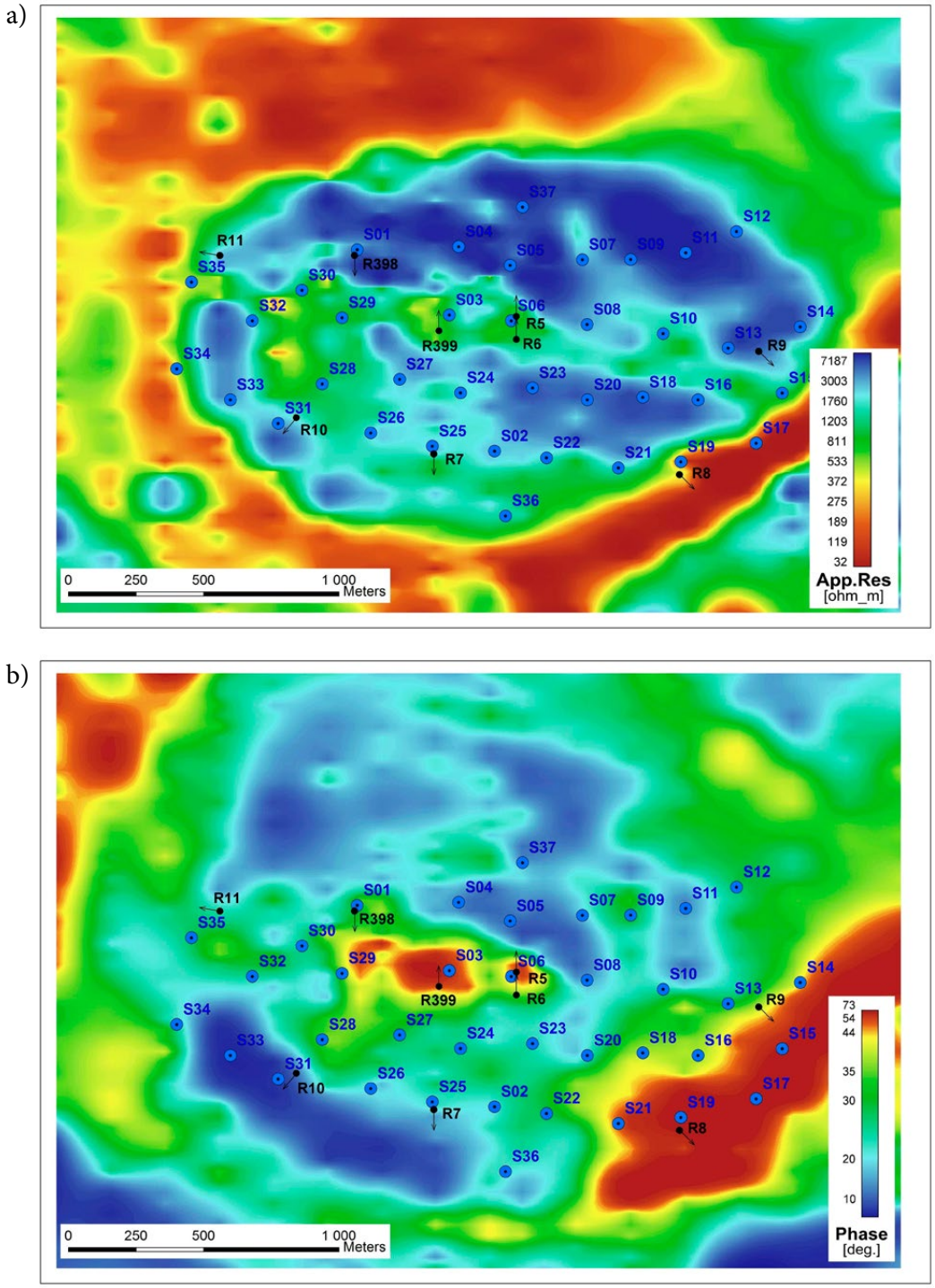

Fig. 11. AMT array on ground VLF-R (a) apparent resistivity and (b) phase maps that show surface conductors in the area. The frequency of the VLF-R transmitter was 23.4 kHz (station DHO). Black arrows show the drill holes in the area. Blue dots show the locations of the AMT sites.

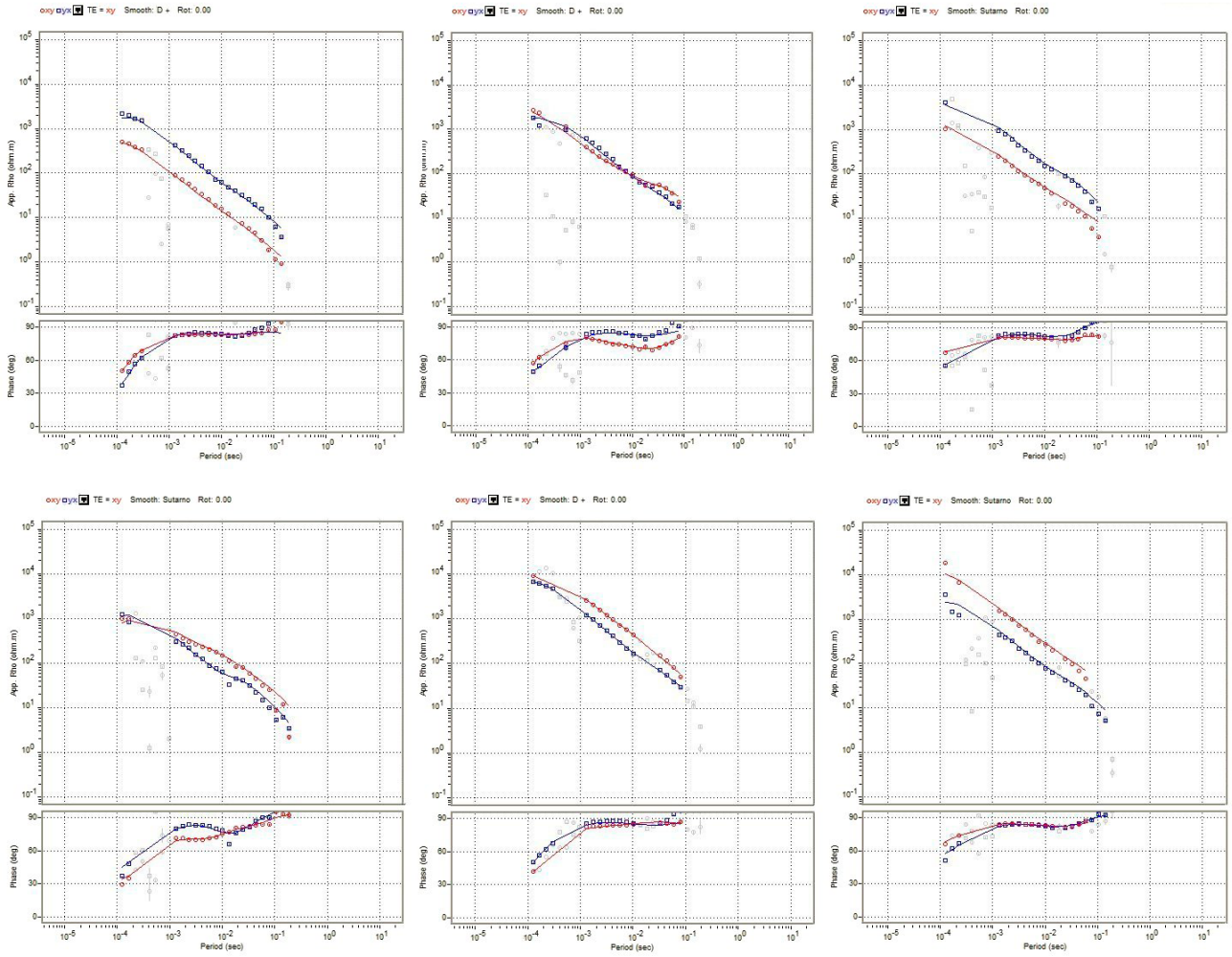

Fig. 12. AMT apparent resistivity and phase curves from the Sotkavaara intrusion. XY and YX data are in the measurement (geomagnetic) direction (data rotation = 0). Therefore, XY (red) curves are calculated from the N–S electric field and E–W magnetic field components, and vice versa for the YX (blue) curves.

Figure 13 presents impedance phase maps (XY and YX) of AMT array data at the frequency of 8000 Hz. For AMT, the 400 m thick intrusion is a relatively shallow target and a high visualization frequency was thus chosen. An anomalous XY phase is detected in the central part of the array at sites S03 and S06 and in the southeastern part of the array. The same phase anomalies were clearly visible in VLF-R phase map (Fig. 11b).

The AMT sounding data are dependent on the measurement direction, which is usually caused by 2D and 3D effects of the electrical conductivity structure. The data can be rotated in any desired direction, since two perpendicular components have been measured simultaneously. This means that 1D modelling of single polarization XY or YX data leads to different results. Various rotationally independent parameters of the impedance tensor have been developed, such as the geometric average of the impedance tensor. These parameters are termed invariants and mathematically some of them are various averages calculated over all possible measurement directions. The use of invariant data is strongly recommended in 1D modelling, because single polarization 1D inversions of real (3D) data bias the results. Figure 14 shows the apparent resistivity invariant at two frequencies. Low apparent resistivity values are encountered in the southeastern part of the array and also in the middle of the array.

Usually, the vertical magnetic field component, B_z, is measured together with the horizontal magnetic and electric field components (see equation 2), and this was also the case in the Sotkavaara measurements. The measurement of B_z enables processing of the transfer function between the horizontal magnetic field components (B_x, B_y) and the vertical magnetic field component (B_z).

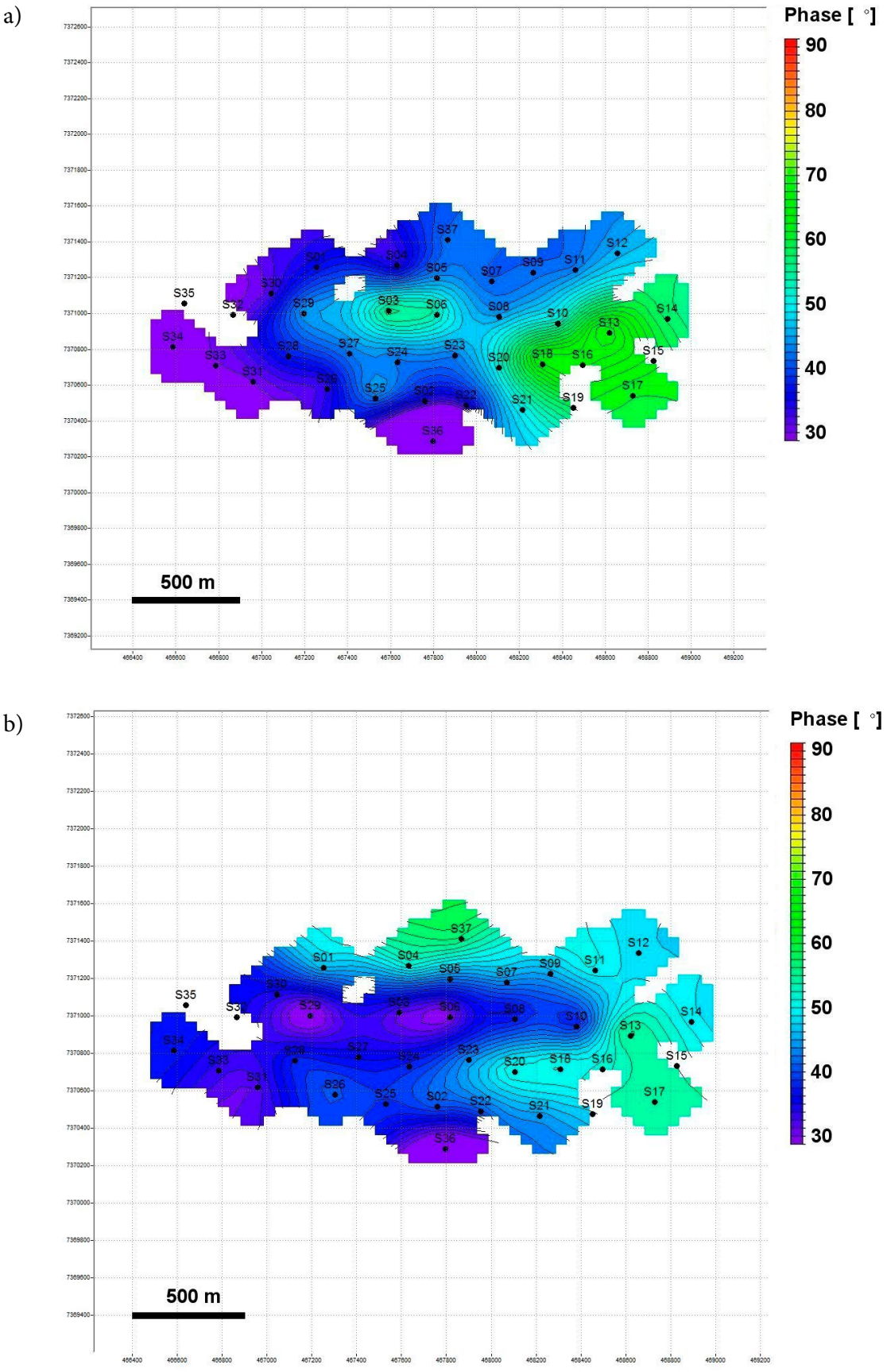

Fig. 13. AMT array impedance phases at 8000 Hz: (a) XY and (b) YX phase.

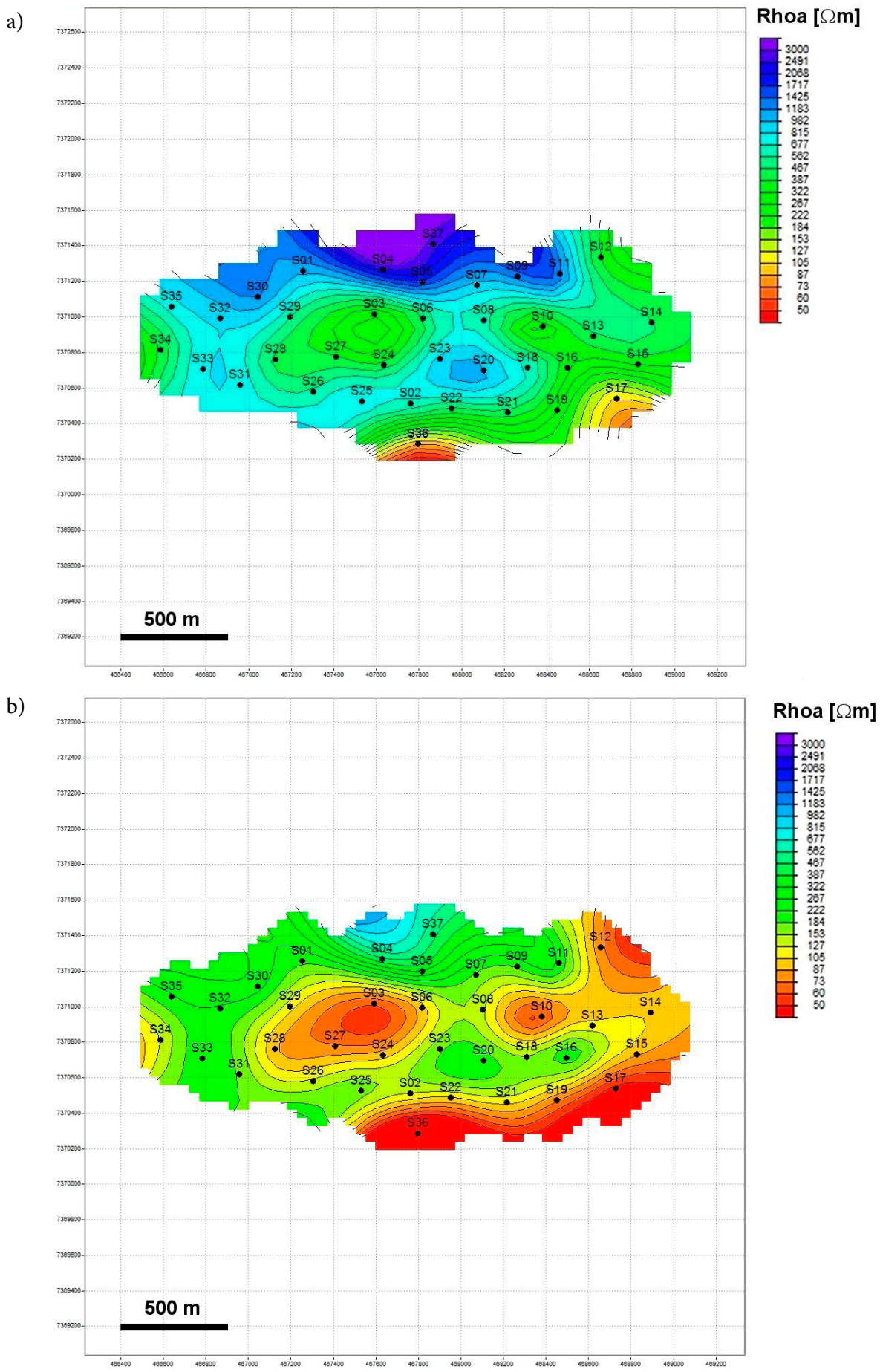

Fig. 14. Determinant average of the apparent resistivity at (a) 750 Hz and (b) 125 Hz.

Graphically, this transfer function is displayed via an induction vector that has both direction and length and it points towards good conductors. For the Sotkavaara case, the measured induction vectors clearly display a conductor around the intrusion (Fig. 15), which is also evident in airborne and ground VLF-R maps.

1D inversion of invariant apparent resistivities and phases was carried out, revealing a resistive upper part and conductive lower part of the intrusion. A shallower conductivity anomaly that coincides with the observed VLF-R phase anomaly (Fig. 11b) was detected in the middle of the array. However, to date, drillings have only revealed a thin sulphide vein that is not thick enough to explain electromagnetic conductivity anomalies.

The measurements and drillings show that the intrusion is three-dimensional. Therefore 3D forward modelling was carried out to fit the main features of the AMT data. Figure 16 shows a perspective view of the 3D model. The shape of the electrical conductivity model follows the 3D magnetic inversion and drilling results. Predicted Tipper responses are presented in Figure 17. The impedance tensor contains four complex elements at each frequency. Due to the many parameters, it is difficult to fit all data simultaneously using forward modelling. However, the model shown in Figure 16 roughly predicts the measured off-diagonal impedances. The next phase will be the implementation of 3D inversion techniques.

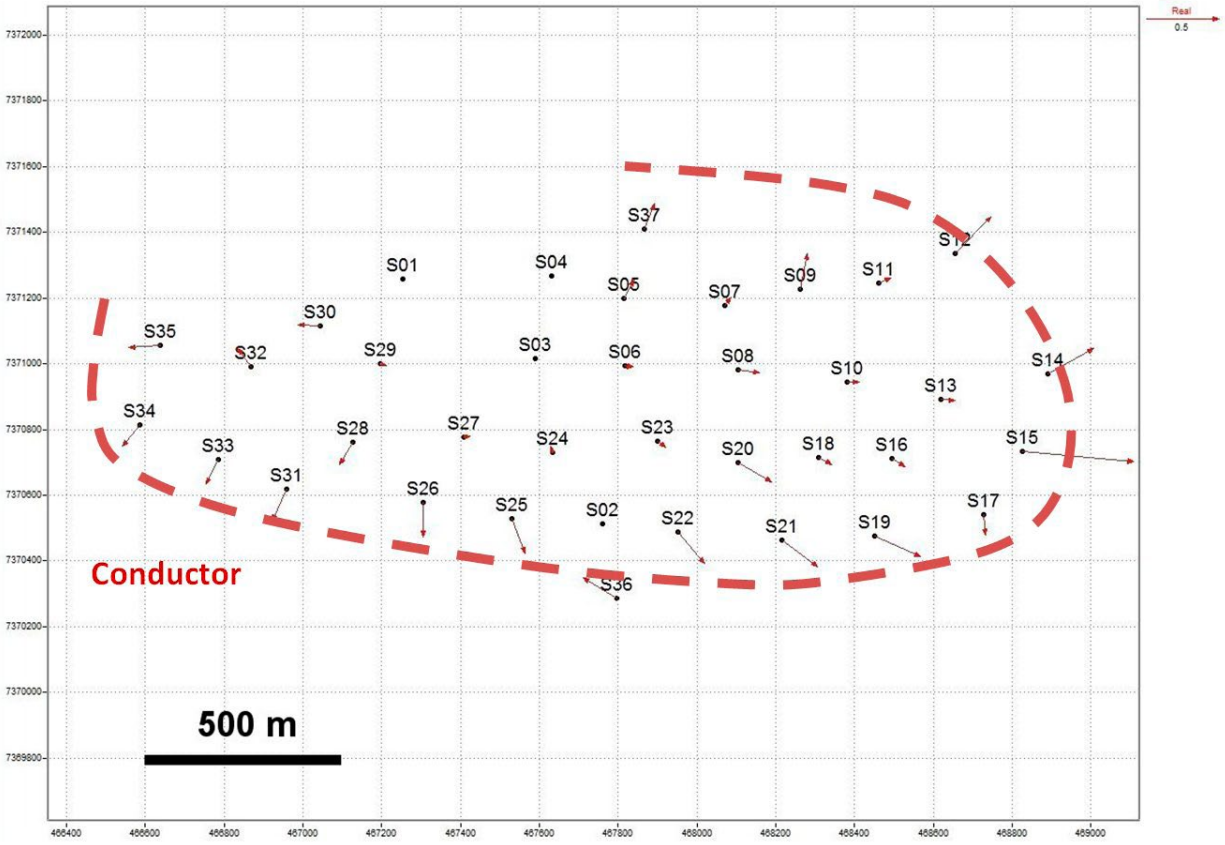

Fig. 15. Processed Re induction vectors at 230 Hz. The vectors show a conductor around the Sotkavaara intrusion.

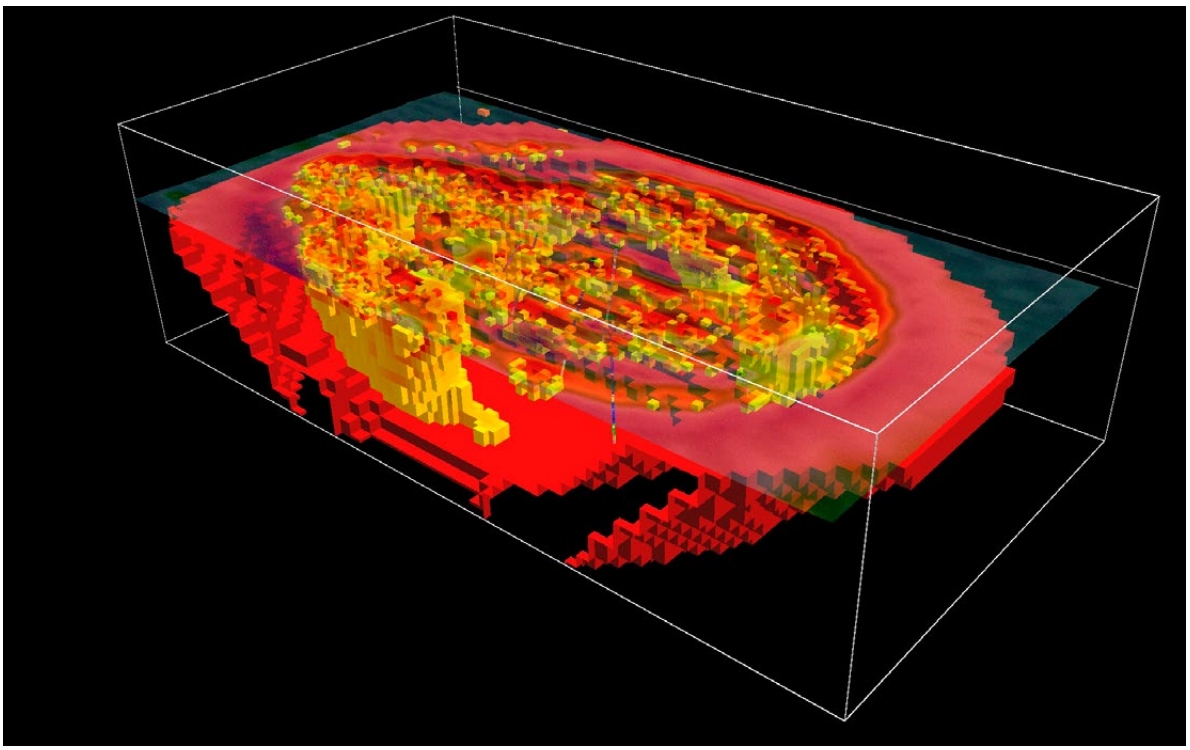

Fig. 16. Integrated 3D magnetic (yellow) and electrical conductivity model (red) of the Sotkavaara intrusion. Frame dimensions 3000 m x 1800 m x 850 m.

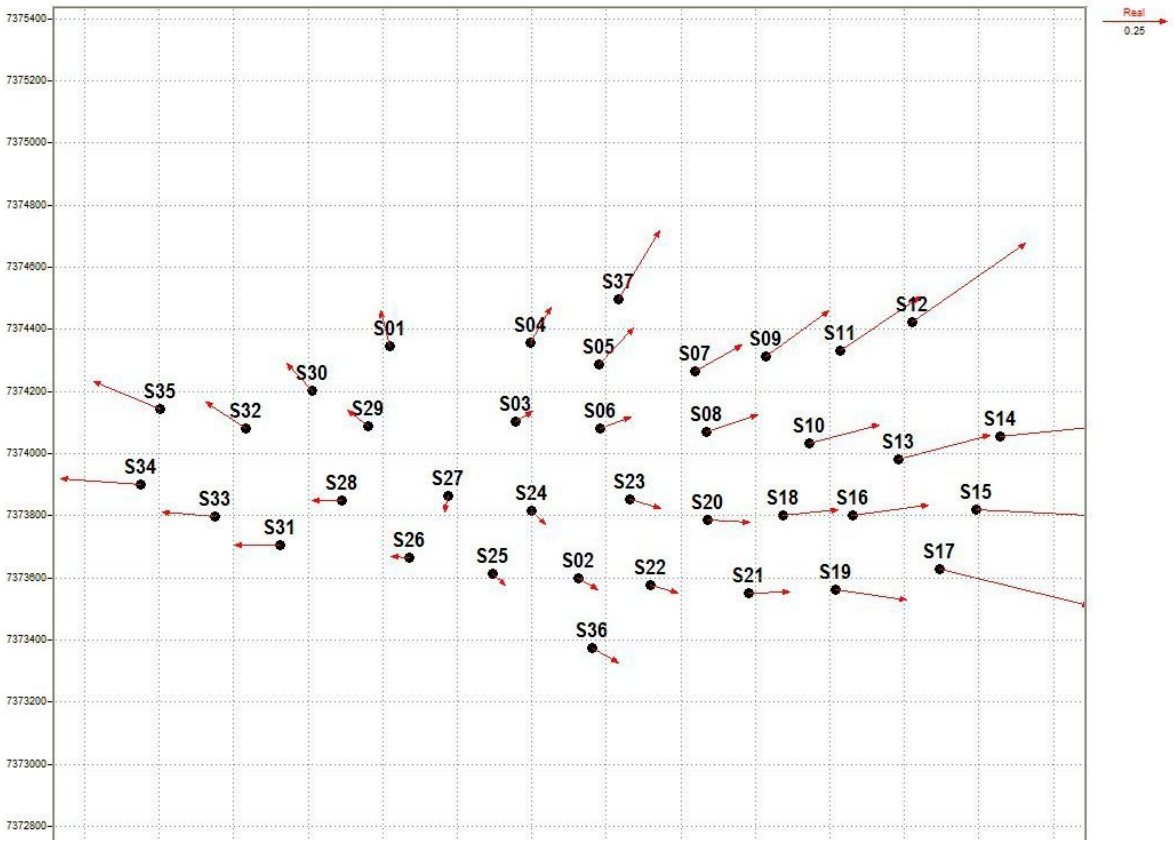

Fig. 17. Predicted Re induction vectors at 230 Hz.

CONCLUSIONS

New tensor AMT equipment has been implemented at the Geological Survey of Finland. Field tests show that 15 min is an adequate recording time for good quality AMT data in the frequency range of 1–10 000 Hz and night time recordings are required to achieve good quality data in the frequency range of 1000–5000 Hz. The use of a remote reference station proved to be essential in the entire AMT frequency range. To enable effective surveying, several practical field protocols were justified, two field crews were trained and equipment was tailored in the project. To speed up measurements, metal sticks were assessed as electrodes and preliminary results encourage the use of the sticks when measuring frequencies higher than 1 Hz. However, this result needs to be confirmed by more extensive testing, because polarization effects can be difficult to recognize. The field example yielded new data from an array survey arranged in the Rovaniemi area. The constructed rough 3D forward model was able to fit the main features of Tipper data and off-diagonal elements of the impedance tensor data.

REFERENCES

Bedrock of Finland – DigiKP. Digital map database [Electronic resource]. Espoo: Geological Survey of Finland [accessed 10.10.2014]. Version 1.0. Available at: http://www.geo.fi/en/bedrock.html

Berdichevsky, M. N. & Dmitriev, V. I. 2008. Models and Methods of Magnetotellurics. Springer. 563 p.

Cagniard, L. 1953. Basic theory of the magneto-telluric method of geophysical prospecting, Geophysics 18, 605–635.

Farquharson, C. G. & Craven, J. A. 2008. Three-dimensional inversion of magnetotelluric data for mineral exploration: An example from the McArthur River uranium deposit, Saskatchewan, Canadian Journal of Applied Geophysics 68, 450–458.

Gamble, T., Goubau, W. & Clarke, J. 1979. Magnetotellurics with a remote magnetic reference. Geophysics 44, 53–68.

Garcia, X. & Jones, A. G. 2002. Atmospheric sources for audio-magnetotelluric (AMT) sounding, Geophysics 67(2), 448–458.

Heinson, G. & White, A. 2005. Electrical resistivity of the Northern Australian lithosphere: Crustal anisotropy or mantle heterogeneity? Earth and Planetary Science Letters 232, 157–170.

Lahti, I., Korja, T., Smirnov, M., Vaittinen, K., Sandgren, E., Niiranen, T. & Nykänen, V. 2012a. 3-D imaging of the Central Lapland Greenstone Belt using magnetotelluric and seismic data. In: EGU General Assembly 2012, Vienna, Austria, 22-27 April 2012. Geophysical Research Abstracts. (Electronic publication)

Lahti, I., Korja, T., Smirnov, M., Niiranen, T., Nykänen, V. & Sandgren, E. 2012b. Electrical structure of the Central Lapland Greenstone Belt, Northern Finland: Interpretation with other geophysical results and geological implications. Book of abstracts. 21st EM Induction Workshop. Darwin, Australia, 25-31 July 2012.

Lakanen, E. 1986. Scalar-AMT applied to base metal exploration in Finland. Geophysics, 51, 1628–1646.

Lanne, E. 2000. Audiomagnetotelluuriset testimittaukset Koillismaalla vuonna 1998. Geological Survey of Finland, archive report Q18/3543/2000/1/24.33, 7 p. (in Finnish)

Pedersen, L. B. & Engels, M. 2005. Routine 2-D inversion of magnetotelluric data using the determinant of the impedance tensor. Geophysics 70, G33–G41.

Rodi, W. L. & Mackie, R. L. 2001. Nonlinear conjugate gradient algorithm for 2-D magnetotelluric inversion. Geophysics 66, 174–187.

Siripunvaraporn, W. & Egbert, G. 2000. An efficient data-subspace inversion method for 2-D magnetotelluric data. Geophysics 65, 791–803.

Smirnov, M., Korja, T., Dynesius, L., Pedersen, L. B. & Laukkanen, E. 2008. Broadband magnetotelluric instruments for near-surface and lithospheric studies of electrical conductivity: a Fennoscandian pool of magnetotelluric instruments. Geophysica 44 (1–2), 31–44.

Strangway, D. W., Swift, C. M. & Holmer, R. C. 1973. The application of audio-frequency magnetotellurics (AMT) to mineral exploration. Geophysics 38, 1159–1175.

Tikhonov, A. N. 1950. Determination of the electrical characteristics of the deep strata of the Earth's Crust, Dok. Akad. Naut., USSR, 73, 295–297.

Törmänen, T., Huovinen, I. & Konnunaho, J. 2014. New type of low-sulphide PGE-reef of the Sotkavaara pyroxenite intrusion, Rovaniemi, Northern Finland. In: Lauri, L. S., Heilimo, E., Leväniemi, H., Tuusjärvi, M., Lahtinen, R. & Hölttä, P. (eds) Current Research: 2nd GTK Mineral Potential Workshop, Kuopio, Finland, 6–7 May 2014. Geological Survey of Finland, Report of Investigation 207. 161 p.

Tuncer, V., Unsworth, M. J., Siripunvaraporn, W. & Craven, J. A. 2006. Exploration for uncon-formity-type uranium deposits with audiomagnetotelluric data: A case study from the McArthur River mine, Saskatchewan, Canada. Geophysics 71, B201–B209.

Türkoglu, E., Unsworth, M. & Pana, D. 2009. Deep electrical structure of northern Alberta (Canada): Implications for diamond exploration. Canadian Journal of Earth Sciences 46, 139–154.

Wannamaker, P. & Doerner, W. 2002. Crustal structure of the Ruby Mountains and southern CarlinTrend region, Nevada, from magnetotelluric data. Ore Geology Reviews 21, 185–210.